VERTICAL MOTION, DIVERGENCE, AND VORTICITY IN THE TROPOSPHERE OVER THE CARIBBEAN, AUGUST 3–5, 1963

M. A. LATEEF

National Hurricane Research Laboratory, IAS, ESSA, Miami, Fla.

ABSTRACT

Vertical motion, divergence, and vorticity have been computed at points over a grid covering the Caribbean and adjoining areas and at seven levels (1000 to 100 mb.) for the period August 3 to August 5, 1963. The synoptic situation during the period was marked by the westward passage of a low-level easterly wave underneath an extensive upper-level anticyclone and the presence of an upper-tropospheric cyclone over the western Caribbean.

Vertical velocities were evaluated from solutions to finite-difference approximations of the pressure-differentiated form of the continuity equation, with suitable boundary conditions. Computed values of divergence and vorticity associated with the easterly wave and the upper-level cyclone compare favorably with those reported in certain previous independent investigations. The computed vertical motion patterns appear realistic though the absolute magnitudes may be in error.

Estimates of the magnitudes of terms in the vorticity equation indicate that the local time-change term is the largest, followed in order of magnitude by the horizontal advection of vorticity and the convergence terms. Vertical transport of vorticity and twisting terms are relatively small. Computed values of the convergence terms (involving vertical derivatives of ω) are not accurate enough for verification on the basis of correlation coefficients between grid-point values of observed vorticity changes and expected vorticity changes. However, improvement of estimates of expected vorticity changes is noticed in many instances when terms in the vorticity equation are averaged over a sizeable area.

1. INTRODUCTION

Kinematic computations of divergence, vertical motion, and vorticity in the Tropics have been carried out by Landers [5], Rex [8], Endlich and Mancuso [3], and Arnason et al. [1]. Detailed estimates of these parameters were made by Yanai [10] in his case study of the formation of Typhoon Doris of 1958. Using a multi-level balanced model with adiabatic frictionless flow, Krishnamurti and Baumhefner [4] have computed vertical motions in the case of an easterly wave associated in the vertical with an upper-tropospheric cold core Low. The purpose of the present study is to construct a three-dimensional picture of vertical motion, horizontal velocity divergence, and vorticity in the troposphere over the Caribbean with the use of wind data over the existing synoptic station network. The analysis area as well as the grid of computation points, is shown in figure 1. The period chosen for study extended from 0000 GMT August 3 to 0000 GMT August 5, 1963. The synoptic situation during this period comprised a moderately strong wave in the low-level easterlies topped by anticyclonic circulation in the upper levels and an upper-tropospheric cyclone over the western Caribbean. For the purpose of making the results of the computations more understandable, a brief account of the evolution of the wind field at the different levels

during the analysis period is presented in the next section. Detailed descriptions of the wind and temperature fields have been presented previously [6].

2. EVOLUTION OF THE WINDFIELD

The low-level easterly wave was first identifiable as a weak perturbation over Puerto Rico on August 2, 1963. At 0000 GMT August 3, the presence of the wave over Hispaniola was clearly indicated by the lower tropospheric wind field (fig. 2). During the next 12 hr., intensification of the wave disturbance into closed circulation occurred simultaneously at the 1000-, 850-, and 700-mb. levels. Closed circulation extended to the higher (550 and 400 mb.) levels by 0000 GMT August 4 (fig. 3). Weakening of the circulation at all levels seemed to occur by 0000 GMT August 5 (fig. 4). Available data in the vicinity of the vortex indicated subsequent degeneration of the low-level vortex into a wave as the disturbance moved westward into the Gulf of Mexico. The average speed of the wave axis during its passage across the Greater Antilles was about 10 kt. Measured from ridge to ridge, the wave length of the perturbation was about 18 degrees of longitude. Wind reports at various levels close to the central region of the system indicated that the axis of the low-level wave and the associated vortex when present tended
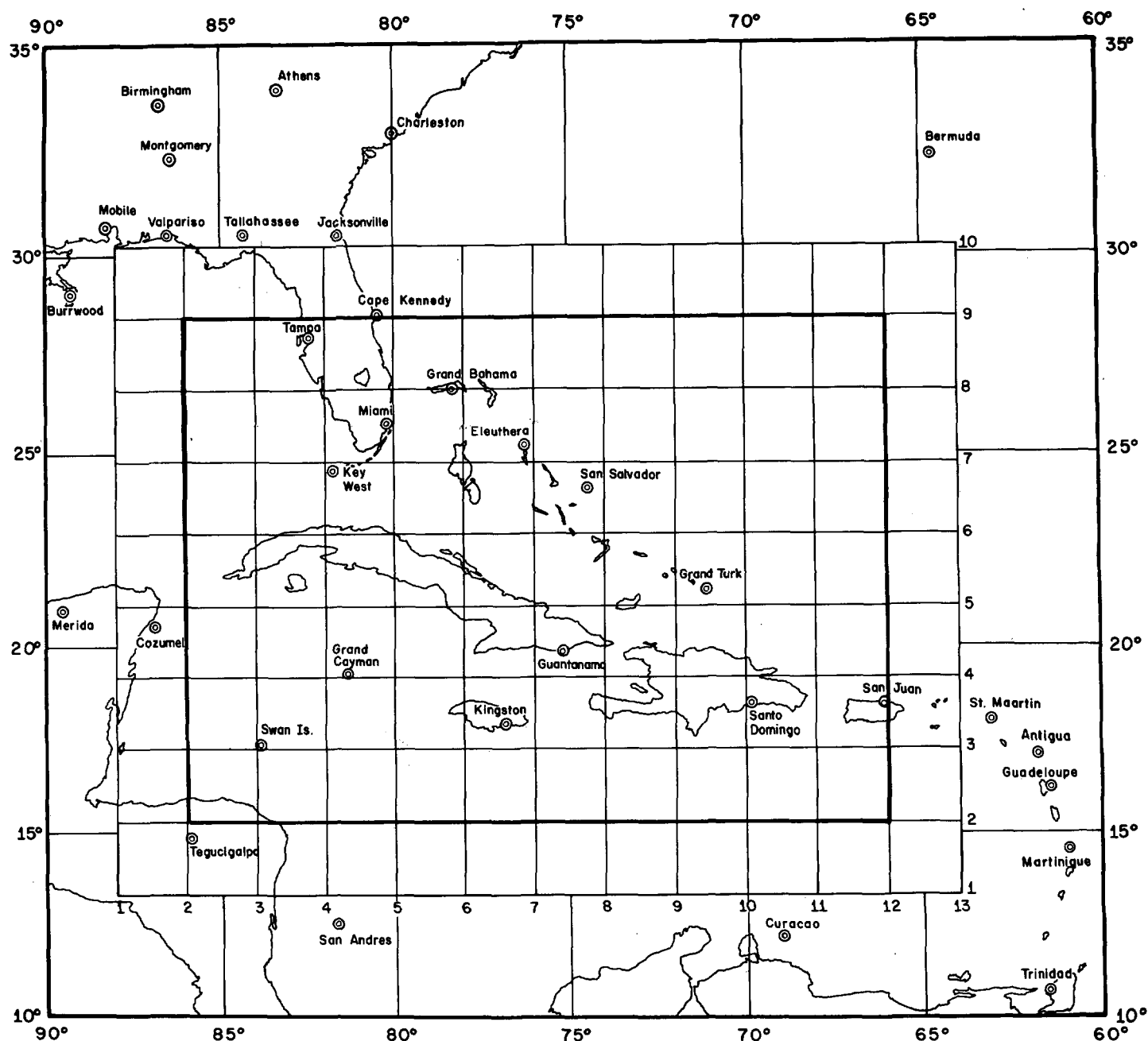
FIGURE 1.—Base map used for analyses and grid over which computations have been made. The perimeter of the grid is shown in heavy lines.

to remain nearly vertical up to about the 600-mb. level and sloped slightly eastward with height above this level.

An upper tropospheric cyclone formed south of Grand Turk at 0000 GMT August 2 and moved southwestward to the position shown at 0000 GMT August 3 over the western Caribbean (fig. 2). During the next 2 days, the cyclone moved westward at the rate of about 4 degrees longitude per day and was out of the analysis area by 1200 GMT August 5. The intensity of the cyclonic circulation increased with height from the 400-mb. level, with maximum intensity generally near the 250-mb. level. The axis of the cyclone remained nearly vertical in the 400–200-mb. layer, during its movement from 0000 GMT August 3

to 1200 GMT August 4, but appeared to slope toward the northwest later.

An extensive anticyclonic circulation at the 250-mb. level persisted over most of the analysis area during the major part of the study period. The central region of the anticyclone was situated near Puerto Rico at 0000 GMT August 3 and moved westward as did the low-level disturbance. In the beginning of the analysis period, the low-level disturbance was located under the western portion of the high-level anticyclone but subsequent differential movements of the systems brought the central region of the anticyclone at 250 mb. almost directly over the low-level disturbance.
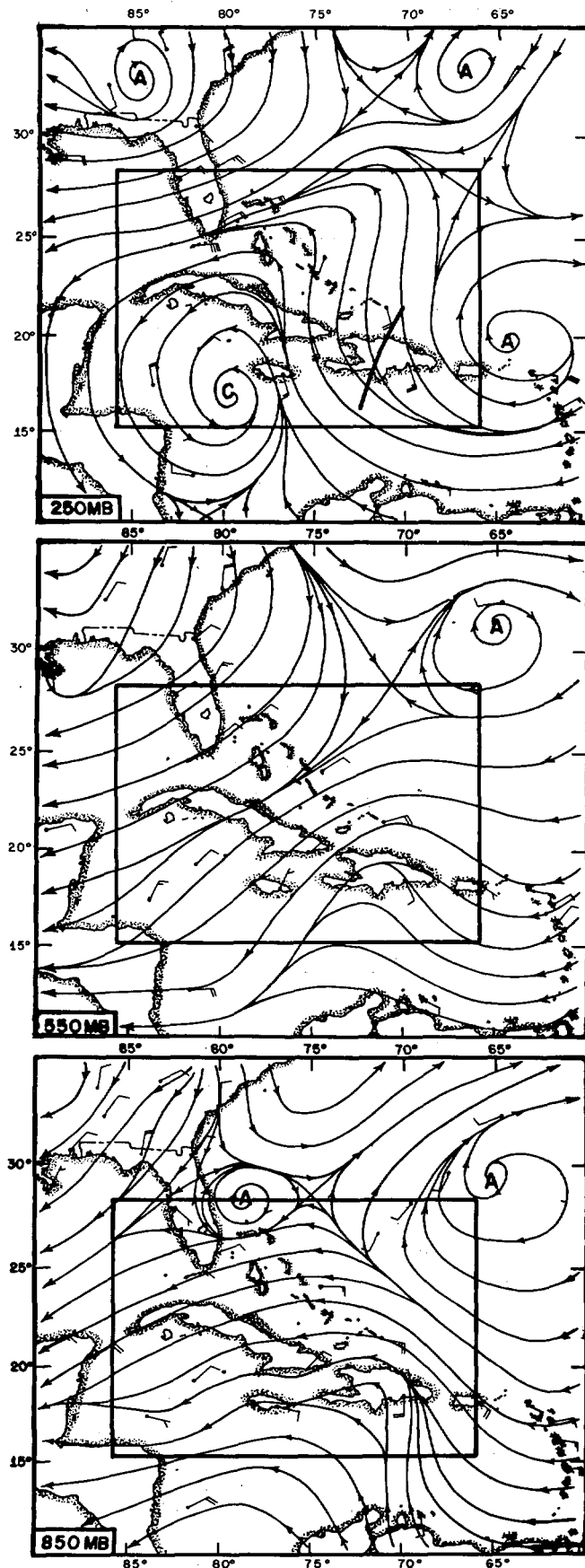
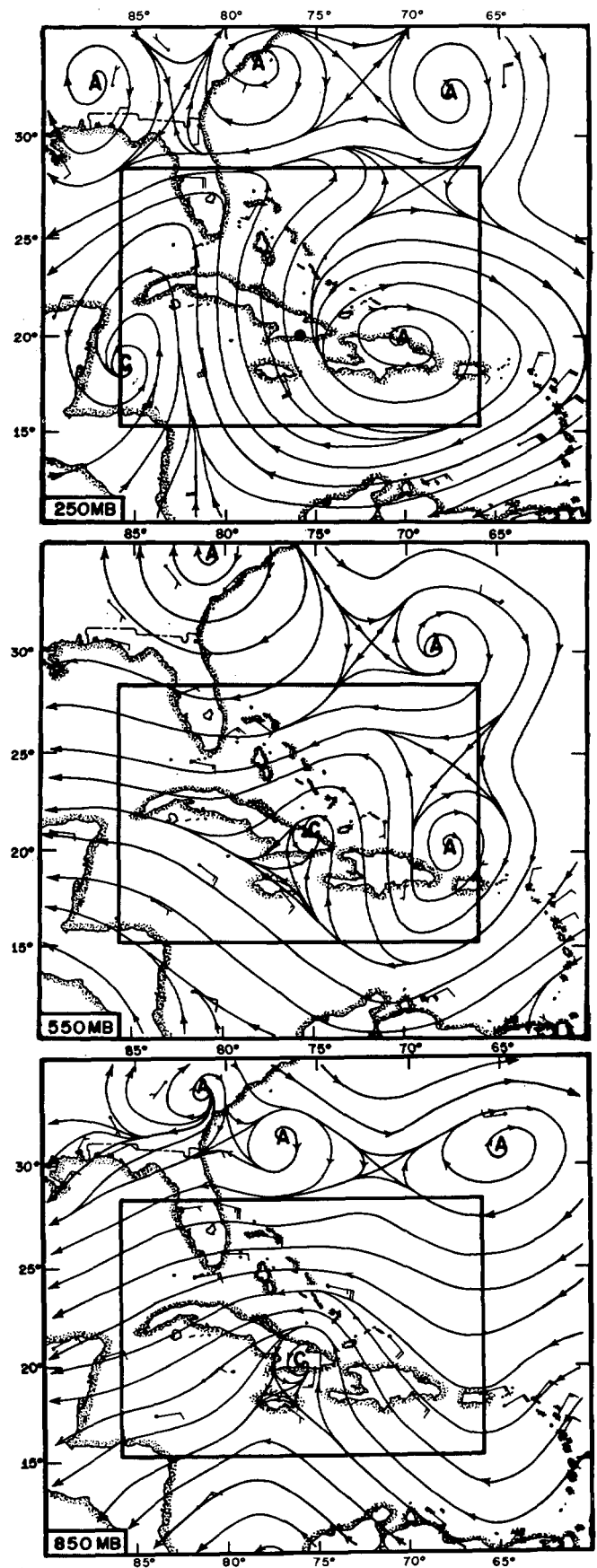FIGURE 2.—Streamline charts at 0000 GMT August 3, 1963.   FIGURE 3.—Streamline charts at 0000 GMT August 4, 1963.
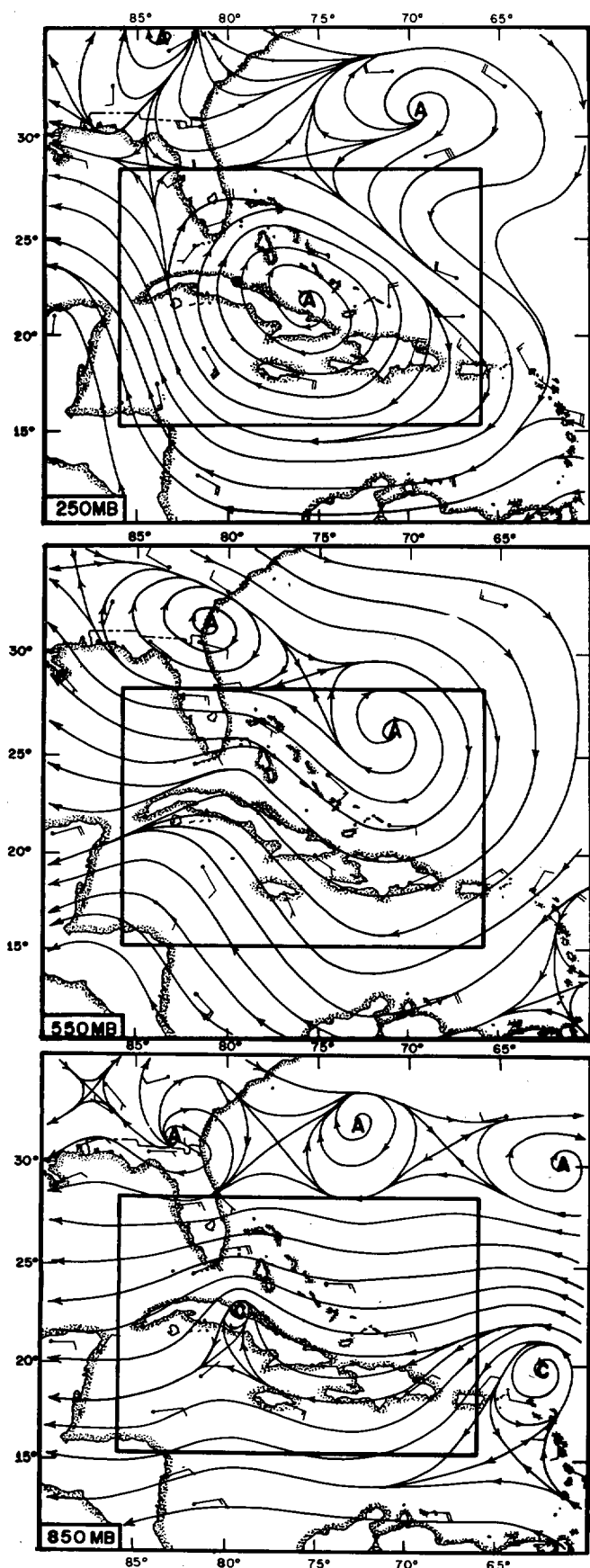
FIGURE 4.—Streamline charts at 0000 GMT August 5, 1963.

The shear zone in the wind field at 250-mb. between the anticyclonic system over southeastern United States and adjoining Atlantic and the anticyclone over the eastern Caribbean was well defined at all map times. Northwestward progression of the shear zone occurred simultaneously with the movement of the low-level disturbance.

There was no evidence of extension of tropospheric systems to the 100-mb. level. The 100-mb. wind field was characterized by a general easterly flow south of the semipermanent anticyclonic belt between latitudes 30° and 35°N.

3. COMPUTATIONAL PROCEDURES

The choice of method of computing vertical motion depends to a large extent on the density and type of available data but is also dictated by the kind of calculations one intends to carry out using the computed values. Computation of vertical motion based on a premise of dry adiabatic process must be regarded as uncertain in areas of upward motion and precipitation. The weak temperature gradients on isobaric surfaces observed in the Tropics introduce uncertainties about the reliability of the computations. Further, the computed values cannot be used for calculating transports of heat and investigating energy transformations associated with the low-level disturbance. Vertical velocities obtained through the conventional kinematic technique, that is, directly from the equation of continuity, $\partial\omega/\partial p = -(\nabla \cdot \mathbf{V})_p$, tend to increase in magnitude with height, mainly due to successive addition in the vertical of errors in divergence values, resulting in a large non-zero value for the net divergence in a column [1, 3]. To obviate this difficulty, a modification of the kinematic technique was adopted in the present investigation such that adiabatic vertical motion values were specified at the 100-mb. level, and vertical velocities at other levels were computed from the pressure-differentiated form of the continuity equation. To the author's knowledge, such a technique for computing vertical motion has not been used in the past.

The base map used for all analyses was a mercator projection true to scale at 22.5°N. The grid consisted of a rectangular array of 130 points with a uniform grid interval of 2 degrees longitude (fig. 1). The input data consisted of appropriate values for the grid distances and the u and v components at each grid point for each map time at the seven levels—1000, 850, 700, 550, 400, 250, and 100 mb. Values of horizontal divergence D, and relative vorticity ζ, were first computed kinematically at each grid point, using average values of wind components along the sides of the 4-degree square surrounding the grid point. The method of computation and the grid dimensions were similar to those adopted by Yanai [10]. In order to eliminate small-scale fluctuations in the divergence and vorticity fields and to retain only the larger scale patterns, the computed fields were subject to a smoothing procedure based on a method described by

Shuman [9]. Comparison of the smoothed fields with the unsmoothed fields showed that, while small-scale features (of the order of two grid intervals) disappeared and the isopleths of zero divergence or vorticity did not shift position appreciably, the maximum and minimum values were reduced to about 70 percent of their initial unsmoothed values.

Vertical velocity $\omega(=dp/dt)$ at each grid point was computed from the relationship

$$\partial^2\omega/\partial p^2 = -\partial D/\partial p \tag{1}$$

on the assumption $\omega=0$ at 1000 mb. Values of ω at 100 mb. were obtained independently by the adiabatic method. Assumption of adiabatic flow at the 100-mb. level cannot introduce any great error in the computed ω-values, in view of the observed high stability at this level and the presence of a reasonably well defined horizontal temperature gradient as compared to lower levels in the area under study [6].

The finite difference approximations corresponding to (1) result in the following set of equations:

$$-2\omega_1+\omega_2 = (D_2-D_0)\Delta p/2 = K_1$$

$$\omega_1-2\omega_2+\omega_3 = (D_3-D_1)\Delta p/2 = K_2$$

$$\omega_2-2\omega_3+\omega_4 = (D_4-D_2)\Delta p/2 = K_3$$

$$\omega_3-2\omega_4+\omega_5 = (D_5-D_3)\Delta p/2 = K_4$$

$$\omega_4-2\omega_5 = (D_6-D_4)\Delta p/2 - \omega_6 = K_5. \tag{2}$$

Here, Δp is the vertical grid interval of 150 mb. D_0 is the divergence at 1000 mb., ω_1 and D_1 are the values at 850 mb. and so on; ω_6 is the known adiabatic value at 100 mb.

The solutions for ω_1, ω_2, ω_3, ω_4, and ω_5 were determined by formulas based on an algorithm described by Young [11]. The solutions are as follows:

$$\omega_5 = -(K_1+2K_2+3K_3+4K_4+5K_5)/6$$

$$\omega_4 = -(K_1+2K_2+3K_3+4K_4)/5 + \tfrac{4}{5}\omega_5$$

$$\omega_3 = -(K_1+2K_2+3K_3)/4 + \tfrac{3}{4}\omega_4$$

$$\omega_2 = -(K_1+2K_2)/3 + \tfrac{2}{3}\omega_3$$

$$\omega_1 = -K_1/2 + \omega_2/2. \tag{3}$$

The set of ω-values over each grid point now represents a field of "revised" horizontal divergence. The revised divergence value at any of the interior levels, 850 mb. to 250 mb., is obtained from the difference between vertical motion values at the two adjacent levels. The revised divergences at 1000 mb. and 100 mb. are given by the relationships

$$D_0^* = \omega_1/75\text{ mb.} - D_1^*$$

and

$$D_6^* = \omega_6/75\text{ mb.} - [D_0^* + 2(D_1^* + D_2^* + D_3^* + D_4^* + D_5^*)]$$

where the D_s^* represent the revised divergence values.

It may be pointed out that the revised divergence values over each grid point represent essentially the original smoothed divergences corrected by an arbitrary constant. This constant arises from the differentiation of the equation of continuity followed by integration of the differentiated equation. The revised values are also subject to truncation errors involved in the set of finite difference approximations (2), as well as in the computation of divergence from the difference in ω-values over a 300-mb. interval. Comparison between the fields of original smoothed divergence and those of revised divergence indicates that, in general, the large-scale patterns do not change position appreciably and the revised values are, on the average, about two-thirds the original smoothed values. The correlation coefficients between the two fields at any level varied from 0.6 to 0.9. In what follows, divergence values will correspond to the revised horizontal divergence values.

The procedure for computing vertical velocities at any level involves differences of the horizontal divergence values at various other levels as well as a fraction of the ω-values at the next higher level. From several examinations it is concluded, that ω-values of the order of 1 mb. hr. $^{-1}$ have the correct sign while values greater than 2 mb. hr. $^{-1}$ are reliable in both sign and order of magnitude.

Since the computed relative vorticities at any level have been found, on the average, to be at least twice the divergence values, the percentage error in vorticity values due to errors in wind speed and direction is less than that in the case of the divergence values. Fairly persistent and large-scale patterns in vorticity are considered reliable.

4. VERTICAL MOTION, DIVERGENCE, AND VORTICITY FIELDS

VERTICAL MOTION AND DIVERGENCE

The evolution of the fields of vertical motion at various levels in the troposphere or the horizontal divergence represented by them was associated with the movement of two major systems over the analysis area. The first system comprised the low-level easterly wave and embedded vortex which moved westward across the Greater Antilles. Throughout its movement, the low-level disturbance existed under an extensive anticyclonic circulation at 250 mb. The second system was the upper-tropospheric cyclone which moved westward across the western Caribbean and the associated shear zone stretching northward from the cyclone center. East to northeasterly flow was present in the low levels beneath this upper tropospheric system.

Figure 5 shows the horizontal divergence and ω-patterns at three selected levels at 0000 GMT August 3. A zone of weak convergence existed to the east and divergence to the west of the wave axis in the low levels. Weak divergence was present in the upper tropospheric layer over the region east of the low-level wave axis. Weak divergence was also indicated in the western portion and convergence in the eastern portion of both the upper-tropospheric cyclonic

circulation in the western Caribbean and the associated shear-line over Cuba and the central Bahamas. Ascending motion east of the wave axis extended from surface to the 400-mb. level and was replaced by descent at and above the 250-mb. level while weak descending motion west of the axis in the low levels changed to weak ascent at and above the 550-mb. level. Continued ascent existed throughout the lower troposphere over the western Caribbean and in the western portion of the upper-tropospheric shear zone while descent occurred over a large area dominated by the low-level easterlies to the north of the wave system and in the southerly flow east of the upper-tropospheric shear zone. Vertical motions over the upper tropospheric cyclone were rather weak and ill-defined at both 400 and 250 mb.

Figure 6 shows the east-west vertical cross-sections of divergence and vertical motion at 1200 GMT August 3, along latitude 21°N. Intensification of low-level convergence has occurred to the east of the wave axis while convergence has also spread to the west of the axis, in conjunction with the formation of a closed circulation within the wave at this time. Divergence in the upper tropospheric levels is associated with the anticyclone centered north of Puerto Rico. The ω-pattern surrounding the wave shows upward motion at all levels with maximum values in the middle troposphere.

Convergence and divergence fields associated with the wave system remained basically unaltered at 0000 GMT August 4, except for some reduction in the magnitudes (fig. 7). Throughout the troposphere, upward motion occurred over a broad region to the east of the wave axis and downward motion elsewhere over the area. Maximum values of ascent were to the east of the low level vortex in the 700–550-mb. layer. Relatively large descent occurred in the lower tropospheric flow west of the wave axis with maximum at the 550-mb. level. Descending motion persisted upwards at and above the 400-mb. level over the eastern portion of the upper-tropospheric cyclonic circulation and over and to the east of the shear zone.

The east-west vertical cross-sections of divergence and ω-fields at 1200 GMT August 4, along latitude 21°N. are presented in figure 8. Except for a slight decrease in the magnitude of convergence at the 1000-mb. surface, no significant modifications to the divergence fields are observed. The reversal with height of convergence to the east and divergence to the west of the low-level axis, to divergence over the upper tropospheric anticyclone and convergence to the east of the shear zone, is clearly depicted. The vertical motion pattern shows one cell of ascent and one of descent extending throughout the troposphere and situated nearly symmetrically with respect to the wave axis.

The horizontal divergence and vertical motion fields at 0000 GMT August 5, when the wave system was in the dissipating stage, are shown in figure 9. Considerable weakening and erosion of the low-level convergence zone to the east of the wave axis occurred while the axis itself lay in a region of divergence in the lower troposphere

topped by convergence in the upper troposphere. Divergence associated with the 250-mb. anticyclone tended to be confined to the southeastern portion of the anticyclonic circulation. Weak ascending motion occurred throughout the troposphere over a region some distance to the east of the wave axis and descending motion elsewhere over the analysis area.

In general, the absolute magnitudes of divergence values reached a minimum in the 550–400-mb. layer. Convergence values to the east and divergence values to the west of the wave axis were usually at a maximum at the 1000-mb. level and decreased in magnitude with height in the lower troposphere. Maximum convergence values ranged from about 10^{-5} sec.$^{-1}$ in the formative stage of the vortex pattern to about 4×10^{-6} sec.$^{-1}$ later when the wave was propagating as a steady-state system. Maximum divergence values to the west of the wave axis were about 5×10^{-6} sec.$^{-1}$ during most of the period. Divergence in the low level easterly flow north of the wave system was also a maximum at 1000 mb. with values about 8×10^{-6} sec.$^{-1}$ at all map times. The level of maximum divergence values in the upper tropospheric layer east of the wave axis varied from map to map. Maximum divergence values of the order to 5×10^{-6} sec.$^{-1}$ were computed at 100 mb. on two occasions. There was no appreciable variation with height of the magnitudes of convergence values associated with the upper-tropospheric wind shear zone, average values being of the order of 2×10^{-6} sec.$^{-1}$ Available convergence values associated with the upper-level cyclone in the western Caribbean indicated maximum magnitudes of the order of 5×10^{-6} sec.$^{-1}$ in the 400–250-mb. layer in the eastern sector of the circulation.

Largest values of upward motion in the middle troposphere to the east of the wave axis ranged from about 3 mb. hr.$^{-1}$ ($=1$ cm. sec.$^{-1}$) on most occasions to about 7 mb. hr.$^{-1}$ ($=2.8$ cm. sec.$^{-1}$) during the intensification stage at 1200 GMT August 3. Maximum values of descent, also at one or more of the mid-tropospheric levels to the west of the wave axis, ranged from about 5 mb. hr.$^{-1}$ ($=1.5$ cm. sec.$^{-1}$) to 8 mb. hr.$^{-1}$ ($=3.2$ cm. sec.$^{-1}$). The absolute magnitudes of vertical velocities at 100 mb. ranged from 0 to 0.4 mb. hr.$^{-1}$ during the entire period.

Convergence and divergence were associated with upward and downward motions in the low levels. In the higher levels, convergence and downward motion existed to the east of the shear zone and in the eastern sector of the cyclonic circulation, during most of the period. Upper tropospheric divergence east of the wave axis was associated with descending motion at the initial map time and ascending motion later on.

The computed magnitudes of low-level divergence and vertical motion compare favorably with values presented by Arnason et al. [1] for a low-level perturbation over the Caribbean. The absolute magnitudes of vertical motion at 250 mb. in the vicinity of the cyclone over the western Caribbean agree in general with values computed at 300 mb. by Krishnamurti and Baumhefner [4] in the case of
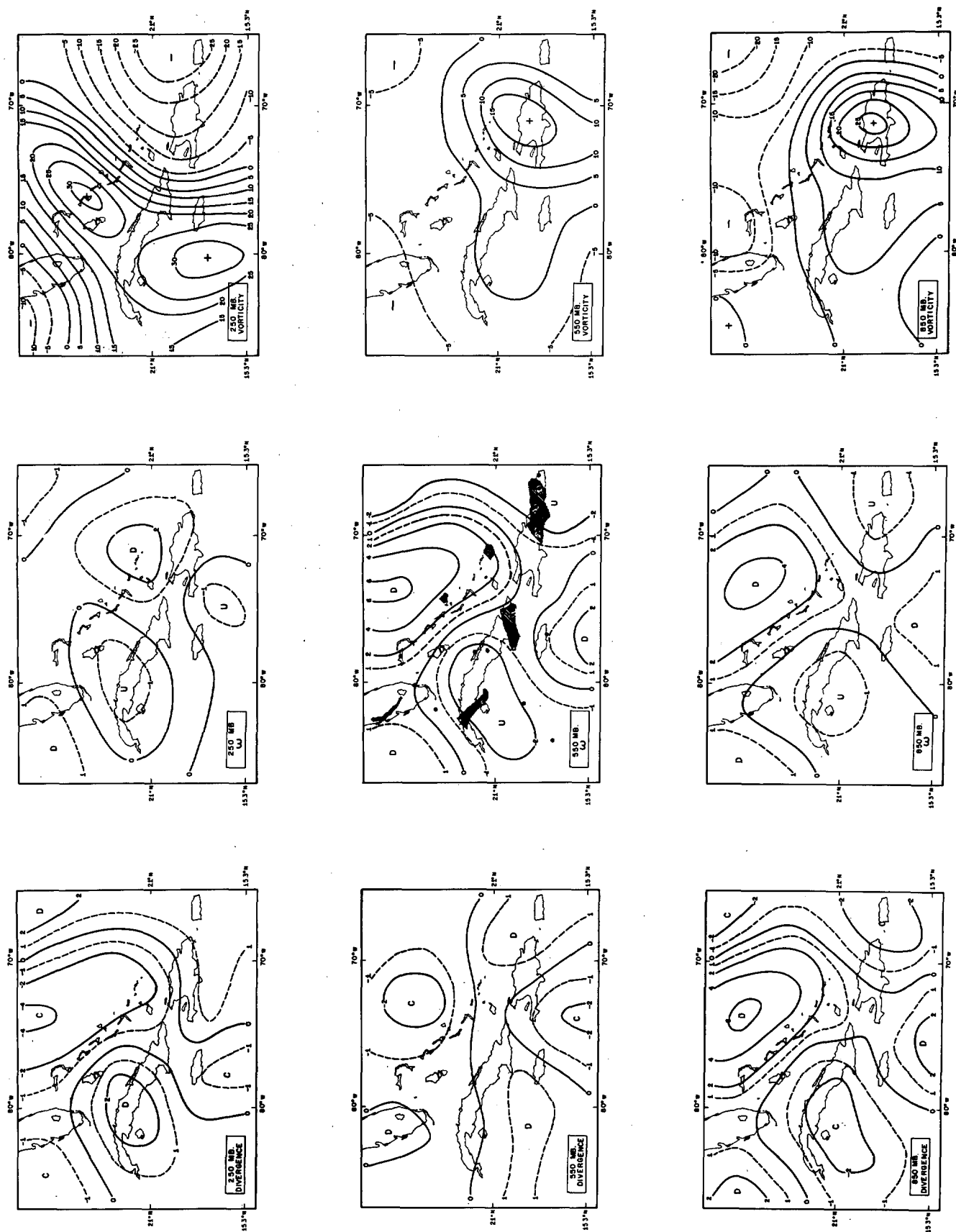
FIGURE 5.—Horizontal divergence, vertical motion, and relative vorticity at 0000 GMT August 3, 1963. Isopleths of divergence and vorticity are labeled in units of 10^{-6} sec.$^{-1}$ Isopleths of vertical motion refer to $\omega = dp/dt$, so that positive values denote downward motion and are labeled in units of mb. hr.$^{-1}$ Cloudiness and precipitation areas are shown by shading in 550-mb. ω-maps.
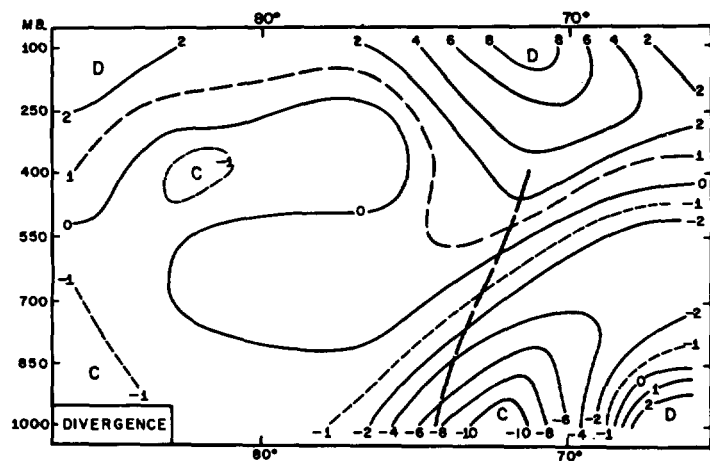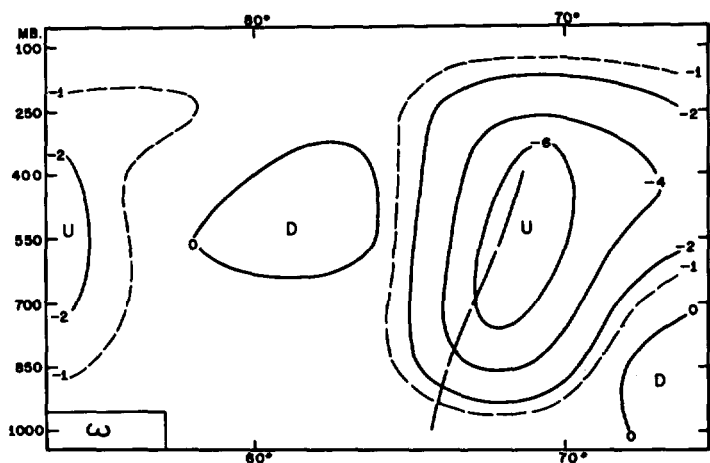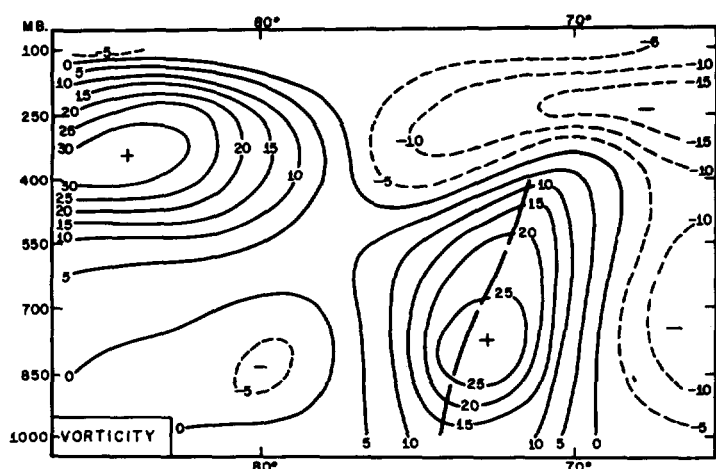
FIGURE 6.—Vertical space sections of divergence (in units of 10^{-6} sec.$^{-1}$), vertical motion (in units of mb. hr.$^{-1}$), and relative vorticity (in units of 10^{-6} sec.$^{-1}$) along latitude 21°N. at 1200 GMT August 3, 1963. Heavy dashed line represents wave axis.

278-472 O - 67 - 6

an upper "cold" Low vertically in phase with a low-level easterly wave.

Qualitative verification of the computed vertical motion fields is indicated in figures 5, 7, 9, and 10. In the absence of satellite cloud observations, available synoptic reports of cloudiness and precipitation have been shown along with the ω-fields at 550 mb. Except at 0000 GMT August 4, the agreement between regions of large-scale upward motion and of precipitation is good. Downward motion in the eastern sector of the upper-level cyclone over the western Caribbean corresponded to reports of little or no convective systems in the area.

RELATIVE VORTICITY

The horizontal and vertical distribution of relative vorticity during the period are shown in figures 5 to 9. At the wave stage, at 0000 GMT August 3, maximum relative vorticity was situated at the crest of the wave in the low levels, with the largest value of 27×10^{-6} sec.$^{-1}$ at the 850-mb. level. During the formation 12 hr. later of a closed circulation within the wave, an increase of relative vorticity was observed at 1000 and 550 mb. with no marked changes in values at 850 and 700 mb. Computations at subsequent map times indicated no significant variations in the patterns of relative vorticity at the low levels. Maximum relative vorticity was present just north of the center of the low-level vortex with the largest values of the order of 30×10^{-6} sec.$^{-1}$ at 850 mb. Weakening of the low-level disturbance at 0000 GMT August 5 was accompanied by decrease in relative vorticity values.

Negative relative vorticity existed over the low-level disturbance, in association with the anticyclonic circulation at the upper-tropospheric levels. Maximum negative values computed near the center of the anticyclone generally increased in magnitude as the system moved westwards, reaching the largest value of the order of -40×10^{-6} sec.$^{-1}$ at 250 mb. at 0000 GMT August 5.

Positive relative vorticity values around the upper-tropospheric cyclone and associated shear zone were generally largest at the 250-mb. level. The maximum value of 57×10^{-6} sec.$^{-1}$ was computed close to the center of cyclonic circulation at 250 mb. at 0000 GMT August 4. This value exceeded that of the Coriolis parameter, 47.9×10^{-6} sec.$^{-1}$ at the same latitude, 19.2°N.

The orders of magnitude of the maximum values of absolute vorticity, of the order of 70×10^{-6} sec.$^{-1}$ in the region of the low-level easterly wave and of the order of 10^{-4} sec.$^{-1}$ near the center of the upper-tropospheric cyclone compare favorably with values obtained by previous investigators in the case of similar perturbations [4, 7].

5. VORTICITY CHANGES

The magnitudes of terms in the vorticity balance over the region under study have been estimated. Comparisons
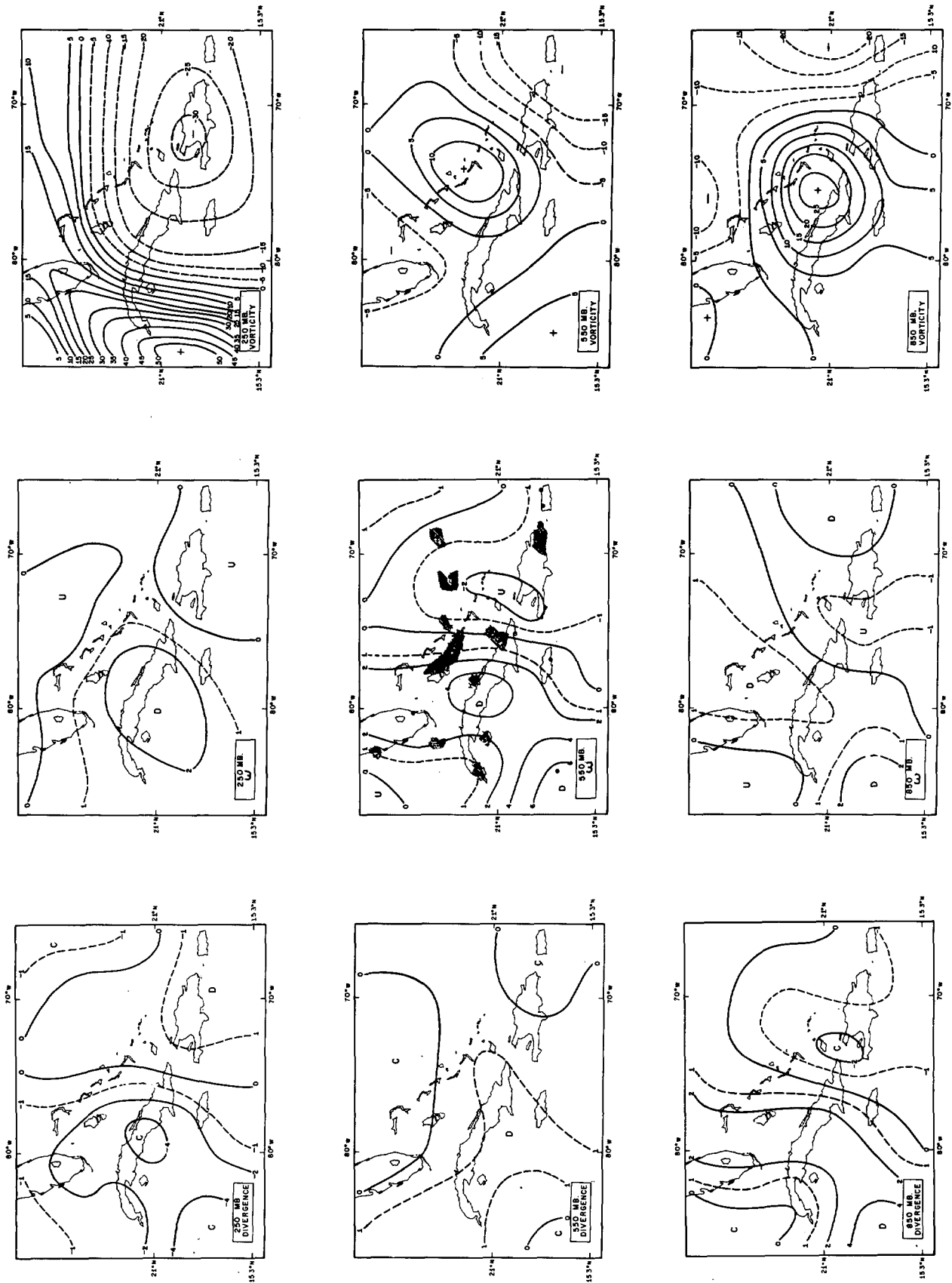
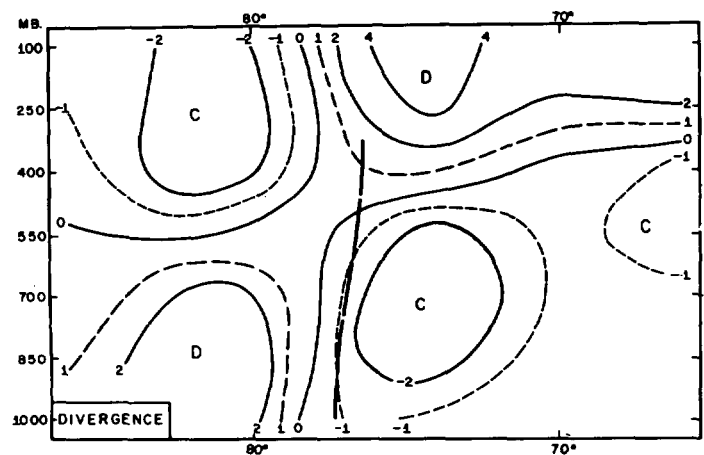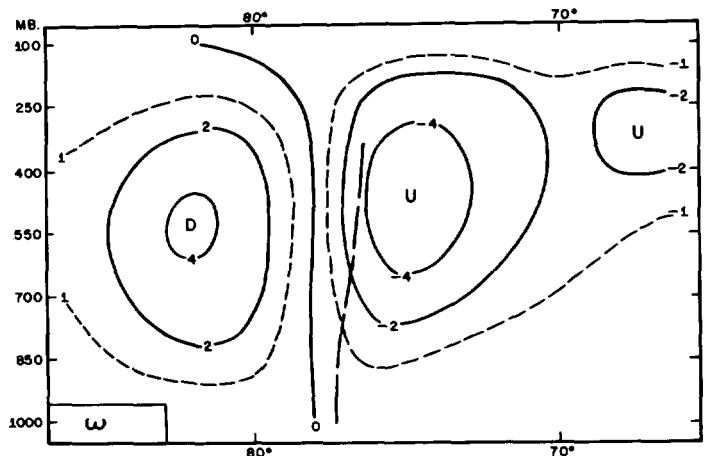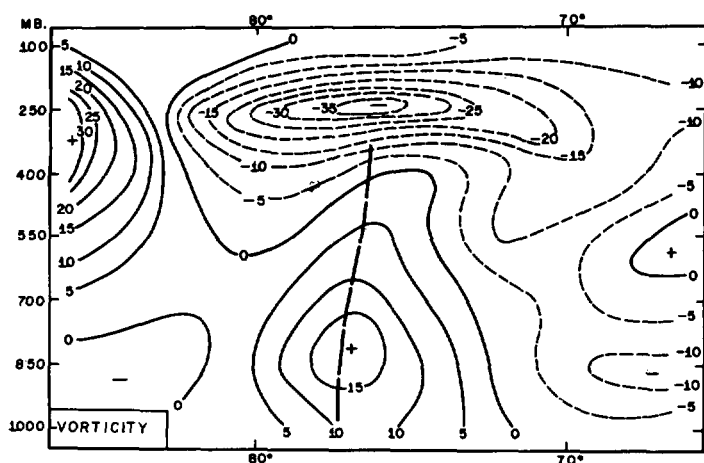FIGURE 7.—Same as figure 5, for 0000 GMT August 4, 1963.

TABLE 1.—RMS *values of terms in the vorticity equation, integrated over Δt ($=24$ hr.), in units of 10^{-6} sec.*[-1]

Term Level	$\Delta\eta(O)$	$(-\mathbf{V}\cdot\nabla\eta)\Delta t$	$(\eta\,\partial\omega/\partial p)\Delta t$	$(-\omega\partial\eta/\partial p)\Delta t$	$(-\mathbf{k}\cdot\nabla\omega\times\partial\mathbf{V}/\partial p)\Delta t$
250 mb.	22.8	15.3	6.8	0.6	0.9
400 mb.	15.7	12.6	5.4	2.3	2.7
550 mb.	10.8	8.5	2.8	1.6	1.8
700 mb.	12.8	10.5	4.8	0.8	1.2
850 mb.	12.3	12.4	6.7	0.3	0.4

FIGURE 8.—Same as figure 6, for 1200 GMT August 4, 1963.

of the independently calculated values of both sides of the vorticity equation,

$$\partial\eta/\partial t = -\mathbf{V}\cdot\nabla\eta + \eta\partial\omega/\partial p - \omega\partial\eta/\partial p - \mathbf{k}\cdot\nabla\omega\times\partial\mathbf{V}/\partial p, \quad (4)$$

have also been carried out, where η is the vertical component of absolute vorticity. These comparisons served as means of testing the accuracy of the computed parameters. Calculations of the "observed" and "expected" changes of vorticity at grid points at the different levels were based on a procedure adopted by Yanai [10]. The "observed" and "expected" local changes in η over a 24-hr. period were given by

$$\Delta\eta(O) \equiv \eta_{t_0+12\,\mathrm{hr.}} - \eta_{t_0-12\,\mathrm{hr.}} \quad (5)$$

$$\Delta\eta(E) \equiv R_{t_0-12\,\mathrm{hr.}}\,(6\,\mathrm{hr.}) + R_{t_0}\,(12\,\mathrm{hr.}) + R_{t_0+12\,\mathrm{hr.}}\,(6\,\mathrm{hr.}) \quad (6)$$

where R is the sum of the terms on the right-hand side of (4).

Table 1 gives the root-mean square values (all maps, all grid points) of terms in the vorticity equation, integrated over 24 hr., for the different levels. The largest is the local time change term, $\Delta\eta(O)$. The second largest is the horizontal advection term and the third largest is the convergence term. Terms representing vertical transport of vorticity and the "twisting" effect are relatively small.

The estimated grid point values of $\Delta\eta(O)$ and $\Delta\eta(E)$ at the different levels were compared with each other on the basis of correlation coefficients and root-mean square errors between them. Comparisons were also carried out in a similar manner between $\Delta\eta(O)$ and horizontal advection term as well as the combined horizontal advection and convergence term, integrated over 24 hr. The results of the comparisons, given in tables 2, 3, and 4, show: (1) the orders of magnitude of the root-mean square errors are nearly as large as those of observed changes in vorticity; (2) in general, the values of the correlation coefficients are good in the lower troposphere, fairly good at 250 mb., and poor at 400 mb.; (3) neglect of the vertical transport and twisting terms does not affect significantly the values of the coefficients or the errors;
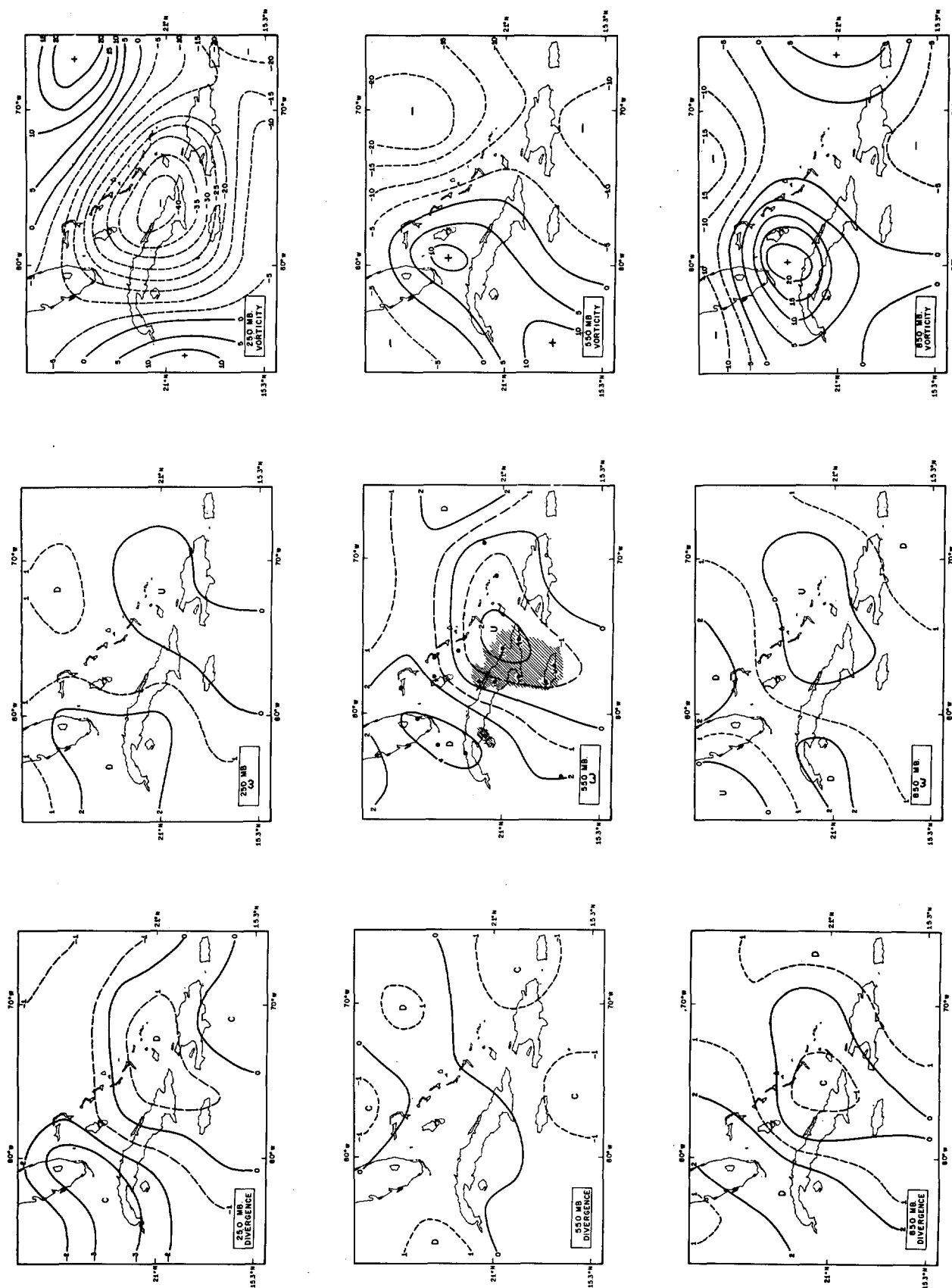
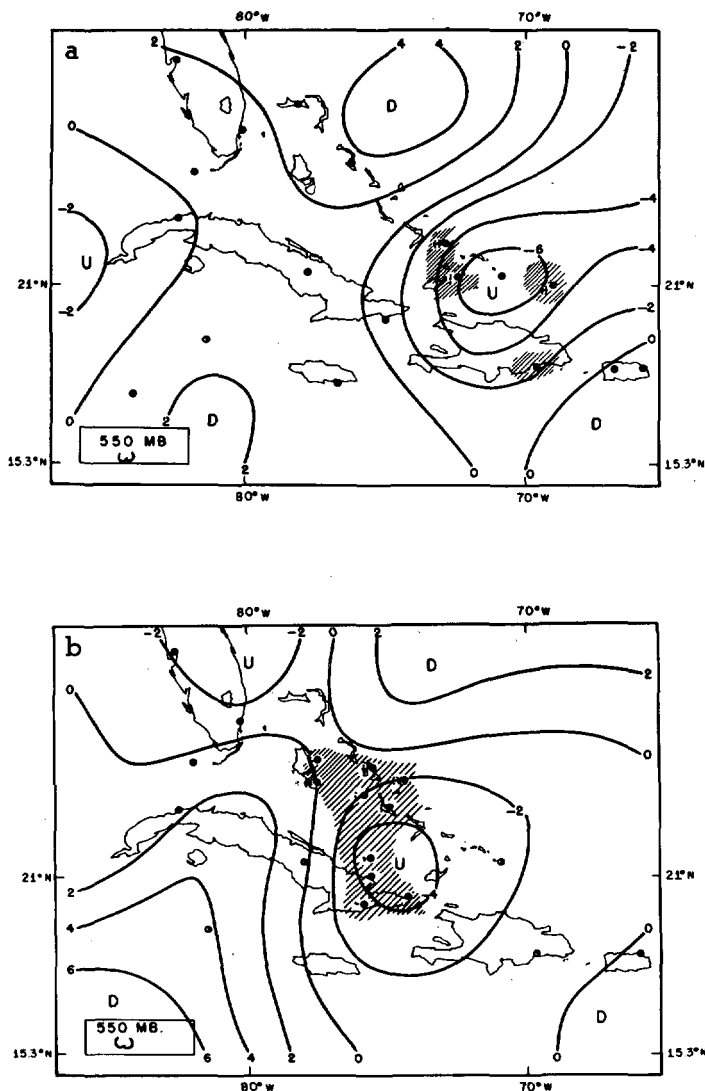FIGURE 9.—Same as figure 5, for 0000 GMT August 5, 1963.

FIGURE 10.—Vertical motion, ω (in units of mb. hr.$^{-1}$) at 550 mb.: (a) 1200 GMT August 3, 1963 and (b) 1200 GMT August 4, 1963.

TABLE 2.—*Correlation coefficients and* RMS *errors* $(10^{-6}$ sec.$^{-1})$ *between* $\Delta\eta(O)$ *and* $(-\mathbf{V}\cdot\nabla\eta)$ *integrated over 24 hr.*

Period / Level	00 GMT Aug. 3 to 00 GMT Aug. 4	12 GMT Aug. 3 to 12 GMT Aug. 4	00 GMT Aug. 4 to 00 GMT Aug. 5	12 GMT Aug. 4 to 12 GMT Aug. 5
250 mb.	0.82(13.10)	0.55(17.71)	0.69(12.89)	0.63(16.73)
400 mb.	0.42(16.76)	0.46(11.38)	0.54(11.99)	0.83(8.76)
550 mb.	0.88(5.48)	0.65(7.02)	0.18(13.22)	0.75(6.75)
700 mb.	0.92(5.67)	0.85(5.97)	0.81(8.39)	0.87(7.39)
850 mb.	0.81(8.87)	0.87(7.64)	0.68(9.40)	0.80(8.64)

and (4) combination of horizontal advection and convergence terms results in improved correlation and reduced error values at the 550-mb. level where the computed

TABLE 3.—*Correlation coefficients and* RMS *errors* $(10^{-6}$ sec.$^{-1})$ *between* $\Delta\eta(O)$ *and* $(-\mathbf{V}\cdot\nabla\eta+\eta\,\partial\omega/\partial p)$ *integrated over 24 hr.*

Period / Level	00 GMT Aug. 3 to 00 GMT Aug. 4	12 GMT Aug. 3 to 12 GMT Aug. 4	00 GMT Aug. 4 to 00 GMT Aug. 5	12 GMT Aug. 4 to 12 GMT Aug. 5
250 mb.	0.59(17.05)	0.38(20.30)	0.64(14.15)	0.58(17.82)
400 mb.	0.28(18.60)	0.26(13.45)	0.55(11.52)	0.80(9.09)
550 mb.	0.91(5.01)	0.69(6.94)	0.22(12.28)	0.76(6.68)
700 mb.	0.88(7.58)	0.77(7.49)	0.70(10.25)	0.69(9.86)
850 mb.	0.65(10.34)	0.77(9.45)	0.53(10.93)	0.53(12.34)

TABLE 4.—*Correlation coefficients and* RMS *errors* $(10^{-6}$ sec.$^{-1})$ *between* $\Delta\eta(O)$ *and* $\Delta\eta(E)$

Period / Level	00 GMT Aug. 3 to 00 GMT Aug. 4	12 GMT Aug. 3 to 12 GMT Aug. 4	00 GMT Aug. 4 to 00 GMT Aug. 5	12 GMT Aug. 4 to 12 GMT Aug. 5
250 mb.	0.58(17.14)	0.37(20.41)	0.67(13.72)	0.60(17.43)
400 mb.	0.25(19.57)	0.19(14.28)	0.44(12.72)	0.72(10.38)
550 mb.	0.82(6.22)	0.66(7.10)	0.11(13.81)	0.69(7.56)
700 mb.	0.85(8.28)	0.77(7.57)	0.70(10.44)	0.72(9.63)
850 mb.	0.63(10.58)	0.77(9.57)	0.53(10.98)	0.53(12.39)

divergence is smallest. At all other levels, correlation coefficients are highest and the root-mean square errors are least between $\Delta\eta(O)$ and the contribution to $\Delta\eta(E)$ from horizontal advection of vorticity alone, over a 24-hr. period.

These comparisons indicate that the computed values of terms in the vorticity equation are not very reliable, at least on a point-by-point basis. In view of the uncertainties inherent in the analysis and interpolation of data and in the numerical approximation procedures, it is difficult to specify the relative magnitudes of the errors in the computations of terms involving ω or its derivatives. The neglect of the frictional term—that is, neglect of vorticity changes due to motions on smaller time and space scales defined by the grid interval—may not be serious enough to alter the results. In a recent investigation of the vorticity budget in the stratosphere, Craig [2] observed that computations of the advection and convergence terms were least reliable on a point-by-point basis, because errors which were random with respect to space could seriously affect the values of these terms. Such errors can, however, be reduced by considering the vorticity budget of an area instead of on a point-by-point basis.

TABLE 5.—*Areal averages, $\Delta\eta(O)$ and advection, convergence terms integrated over Δt (=24 hr.), in units of 10^{-6} sec.$^{-1}$*

Period	Level (mb.)	$\Delta\eta(O)$	$(-\mathbf{V}\cdot\nabla\eta)\Delta t$	$(-\mathbf{V}\cdot\nabla\eta + \eta\partial\omega/\partial p)\Delta t$
00 GMT Aug. 3 to 00 GMT Aug. 4	250	−29.38	−16.86	−14.87
	400	−7.85	−12.87	−11.14
	550	−1.49	−1.87	−1.50
	700	3.63	2.61	3.43
	850	3.75	1.70	2.75
12 GMT Aug. 3 to 12 GMT Aug. 4	250	−28.45	−13.80	−11.98
	400	−9.33	−11.71	−11.36
	550	−7.85	−5.40	−6.85
	700	−4.90	−3.78	−5.19
	850	−2.80	−4.60	−3.82
00 GMT Aug. 4 to 00 GMT Aug. 5	250	−9.67	−6.72	−9.90
	400	−7.89	−7.42	−7.89
	550	−4.33	−6.67	−6.20
	700	−7.33	−7.36	−7.03
	850	−8.28	−8.10	−7.53
12 GMT Aug. 4 to 12 GMT Aug. 5	250	5.76	2.22	2.02
	400	−2.97	−3.97	−3.11
	550	−2.81	−4.39	−3.92
	700	−7.12	−7.29	−5.73
	850	−9.41	−8.00	−8.44

Table 5 shows the average values of $\Delta\eta(O)$ and the average values of the horizontal advection and the combined horizontal advection and convergence terms, over a fixed 5×5 grid inside the basic grid. It is seen that combination of convergence and horizontal advection of vorticity has tended to improve the estimated values of vorticity change, in more than half the number of cases.

6. SUMMARY AND INFERENCES

Vertical motion and divergence, as well as vorticity and magnitudes of terms in the vorticity equation, have been estimated at various levels in the troposphere over the Caribbean, during the period August 3 to August 5, 1963. Vertical velocities and corresponding divergence values were computed by a modified kinematic method, based on solutions to the pressure-differentiated continuity equation. The vertical velocity patterns obtained from the modified kinematic method adopted in the present study appear realistic though the absolute magnitudes may be in error. The magnitudes of vertical velocity are much less than what one would get from the conventional kinematic method but are presumably larger than values based on adiabatic flow. Divergence, vertical motion, and vorticity values associated with the low-level easterly wave and the absolute magnitudes of vertical motion near the central region of the upper-level cyclone compare favorably with those reported in previous independent investigations.

In the low levels, convergence existed with upward motion and divergence with downward motion. A general correlation between the signs of horizontal divergence and vertical motion was not observed in the upper levels. Upper tropospheric divergence east of the wave axis was associated with descending motion initially and ascending motion later on, while convergence and downward motion existed to the east of the upper-level shear zone and the western Caribbean cyclone.

The root-mean square values of the various terms in the vorticity equation, with the frictional term omitted, indicate that the local time change term is the largest, followed in order of magnitude by the horizontal advection of vorticity and convergence terms. The vertical transport and twisting terms are relatively small.

The "revised" divergences represented by the ω-values do not possess sufficient accuracy for verification on the basis of correlations between grid-point values of observed vorticity changes and "expected" vorticity changes, except perhaps, at the 550-mb. level where the divergences happen to be smallest. However, areal averaging of terms in the vorticity equation indicates improvement, in many cases, of estimates of expected vorticity changes when contributions from both horizontal advection and convergence are combined.

REFERENCES

1. G. 'Arnason, K. D. Hage, G. M. Howe, and P. S. Brown, Jr., "Theoretical and Synoptic Studies of Low-Level Tropical Perturbations," *Final Report*, U.S. Weather Bureau, Contract Cwb-10759, The Travelers Research Center, Inc., Hartford, Nov. 1964, 100 pp.
2. R. A. Craig, "The Dynamics of Stratospheric Circulations," *Final Report*, Contract No. AF19(628)–394, Florida State University, Tallahassee, July 1965, 34 pp.
3. R. M. Endlich and R. L. Mancuso, "Objective and Dynamical Studies of Tropical Weather Phenomena," *Final Report*, Contract DA36–039 Sc-89092, Stanford Research Institute, Menlo Park, Calif., Aug. 1963, 47 pp.
4. T. N. Krishnamurti and D. Baumhefner, "Structure of a Tropical Disturbance Based on Solutions of a Multi-Level Baroclinic Model," *Journal of Applied Meteorology*, vol. 5, No. 4, Aug. 1966, pp. 396–406.
5. H. Landers, "A Three-Dimensional Study of the Horizontal Velocity Divergence," *Journal of Meteorology*, vol. 12, No. 15, Oct. 1955, pp. 415–427.
6. M. A. Lateef and C. L. Smith, "A Synoptic Study of Two Tropical Disturbances in the Caribbean," *ESSA Technical Memorandum* IERTM-NHRL 78, Apr. 1967, 33 pp.
7. C. E. Palmer, "Tropical Meteorology," *Quarterly Journal of the Royal Meteorological Society*, vol. 78, No. 336, Apr. 1952, pp. 126–164.
8. D. F. Rex, "Vertical Atmospheric Motions in the Equatorial Central Pacific," *Geophysica*, vol. 6, Nos. 3–4, 1958, pp. 479–501.
9. F. G. Shuman, "Numerical Methods in Weather Prediction: II. Smoothing and Filtering," *Monthly Weather Review*, vol. 85, No. 1, Nov. 1957, pp. 357–361.
10. M. Yanai, "A Detailed Analysis of Typhoon Formation," *Journal of Meteorological Society of Japan*, vol. 39, No. 4, Aug. 1961, pp. 187–214.
11. D. Young, "The Numerical Solution of Elliptic and Parabolic Differential Equations," *Survey of Numerical Analysis*, McGraw-Hill Book Company, Inc., New York, 1962, 584 pp.